Journal of Engineering Science and Technology
Vol. 18, No. 1 (2023) 735 - 750

FINITE ELEMENT BASED PARAMETRIC ANALYSIS OF PMSM FOR ELECTRIC VEHICLE APPLICATIONS

RUPAM, SANJAY MARWAHA*, ANUPMA MARWAHA

Sant Longowal Institute of Engineering and Technology,
Longowal, 148106, Sangrur, Punjab, India
*Corresponding Author: marwaha_sanjay@yahoo.co.in

Abstract

Electric motor plays a major role in an EV (Electric Vehicle) and therefore its design has significant weightage to decide the overall performance of a vehicle. EV's are desired to have less vibration and acoustic noise which in turn enhances the life span of the motor and battery. In this paper, the designing of PMSM (Permanent Magnet Synchronous Motor) for effective propulsion of three-wheeler electric vehicles has been discussed. The cogging torque generated by the permanent magnets and stator teeth causes noise and vibrations in the motor which has been taken care of by varying the embrace factor and magnet thickness. Motor performance has been compared and analysed with different configurations of permanent rotor pole magnets. Parametric analysis is used to increase the electromagnetic torque by taking into consideration the embrace factor and magnet thickness as design variables. Finite Element Method based Ansys Maxwell platform is utilized for the electromagnetic field analysis of PMSM with h-adaptive refinement technique. The designed model offers significant reduction in torque ripples and offers optimum trade-off between efficiency and torque.

Keywords: Electric vehicle, FEM, PMSM, Rotor magnet shape, Torque ripple.

1. Introduction

Currently, energy and environment both have become matters of concern worldwide. With the advancement of urbanisation and industrialization, there is a significant increase in air pollution which is one of the prime factors of global temperature rise. Also, the cost of conventional energy sources is increasing due to its limited availability [1]. Since the adoption of zero emission vehicles (ZEVs) is a matter of time which is either powered by battery, chemically powered or fuel cells [2]. The battery electric vehicle (BEV) performance includes maximum cruising speed, gradeability and acceleration. The electric motor(s) used must have a higher starting torque to accelerate the vehicle. Amongst the propulsion motor(s), permanent magnet synchronous motor (PMSM) is the most prevalent type in use at present because of their high-power density, high torque to inertia ratio, extended speed range, better energy-efficiency, having less weight and due to its compact size [3]. The interior permanent magnet synchronous motor (IPMSM) and surface permanent magnet synchronous motor (SPMSM) both can be considered for the propulsion purpose [3]. The IPMSM can be used in industries where wide speed range operation is desirable. The cogging torque is the result of interaction between permanent magnets on rotor and stator teeth which generates pulsating harmonics in the torque characteristics. To mitigate the pulsating waveforms, some researchers have already explored this area [4, 5].

The choice of the design of the motor reflects many design variations, to govern the dimensions and the materials to be used in the motor. Hence, to accomplish a good and optimum design as per the application area the first thing to observe is the design process. The electromagnetics problems can be solved with computational tools. The field of computational electromagnetism has been revitalized with high-performance systems to save time and costs. Out of the several numerical methods, finite element method (FEM) is best suited to solve low frequency complex domain electromagnetic field problems [6-8]. Optimum design of the machine could be obtained by incorporating finite element adaptivity that establishes a closed loop between pre-processor and post-processor functional elements. Extensive focus on implementation of adaptive finite element technique for designing of motors is picking pace gradually. Many analytical models have been proposed using analytical equations. As reported in literature, the usage of FEM due to its flexibility in complex domains and particularly in designing of different kinds of motor's configuration is increasing over the time [9-14].

It has been observed that researchers have studied and analysed various characteristics of motors used in electric vehicles considering speed, power density, torque and different parameters related to electromagnetic fields. Elamin and Wendling [15] proposed a model of PMSM with rotor skewing technique to mitigate the torque ripple and cogging torque for EV application. Wang et al. [16] proposed the V-shaped IPMSM model with the multi-objective optimization technique to enhance the output torque of the motor. The electromagnetic result analysis has been done with ANSYS Multiphysics simulation.

Bdewi et al. [17] proposed an outer rotor PMSM model for electric vehicles with the multi objective optimization technique. The analysis has been investigated with MagNet software to optimize the slot winding parameters. The optimised model has decreased torque ripple and increment in torque density of the model has been noticed. Mersha et al. [18] proposed the design of PMSM model with ANSYS

Maxwell and co-simulation has been done with ANSYS twin builder and ANSYS Simplorer. Proposed closed controller provided to the motor has enhanced its performance.

Du et al. [19] determined the effect of pole and slot number with the pole arc coefficient on the stress, loss, and temperature of the designed high speed PMSM. Further the simulated results are validated with the experimental results. Murali et al. [20] proposed a model of PMSM for the E-rickshaw and analysed the same with ANSYS Maxwell. The modelling of the vehicle has been done for flat and sloped roads with dynamic equations for the gear type vehicle.

Li et al. [21] proposed outer rotor flux switching permanent magnet machine for light electric vehicle drive system. With the use of sizing equation and finite element method (FEM), 6 stator slots and 19 rotor poles having 188 W and 120 rpm combination are designed for an application. Calculation of magnetic field distribution and machine parameter is done and then performance is analysed by current vector strategy. Chen [22] presented parametric sensitivity analysis on the geometry of the rotor for V-shaped Interior Permanent Magnet Synchronous Motor (IPMSM). Here in detailed manner all the electromagnetic characteristics in low speed and high-speed regions are investigated with improved results.

Zhang [23] proposed to construct a 60kW Interior permanent magnet (IPM) V shaped motor for medium sized electric vehicles under rated operating conditions and overload conditions. The electromagnetic torque, geometric parameters, permanent magnet dimensions and skewing effect implemented with the help of 2D Maxwell software and thermal analysis is done under the same conditions. Ibtissam et al. [24] proposed the design of radial-flux permanent magnet synchronous motor (radial-flux PMSM) by minimizing weight and maximizing torque and efficiency. Here Monte Carlo method is used to optimize the dimensions of the motor to get torque, efficiency and active mass of the motor.

Zhou and Shen [25] studied the effect of asymmetrical flux barriers on cogging torque and ripple torque in an internal permanent magnet synchronous motor with a V-shaped rotor arrangement. Three alternative asymmetric flux barrier models were proposed, and FEM was used to analyse them. Reluctance torque, magnetic saturation electric loads, and back emf harmonics were not affected by the proposed technique. Li et al. [26] proposed a new method which includes superposition concept and subdomain method to determine the cogging torque with rotor eccentricity of the permanent magnet motor. By using Maxwell stress tensor, cogging torque is determined and effectiveness is illustrated on 9slot/8pole and 12slot/10pole motors by FEA. Further this method can be enforced to high stator slot and rotor pole combination.

Han et al. [27] designed IPMSM with a new technique named Box- Behnken. This Permanent magnet of triangle shape is designed to maximize the torque and to minimize the torque ripple. Finite element method is used to determine the position of permanent magnet and within range safety factor. In the past structural based research has been carried out to some extent for enhancing the performance of motors. The effect of pole slot combination on the performance of the motor has been analysed with the help of FEM based tools [28-30].

From the literature survey, it is concluded that the motor has inherent issues regarding cogging torque which is the prime factor for the production of torque

ripples in the moving torque characteristics of PMSM. However, functioning of the motor may be normalized with skewing slots, optimum matching of slots and poles, winding layout etc. It is worth to mention that PMSM has been preferred over BLDC motor in this paper. PMSM has a higher power density, which will help in reducing the size of the motor. Due to low torque repulsion, PMSM got higher and smooth torque with higher efficiency and low noise compared to BLDC motor. If cost of motor is not main consideration, then PMSM is better than BLDC motor in terms of performance and is good to use in electrical vehicles.

This paper contributes the design of the PMSM for the three-wheeler electric vehicle using the finite element method, which is a verified optimization technique to analyse the low frequency electromagnetic field problems. With the help of kinematic dynamic equations, the ratings of the motor have been determined for the Indian Driving Cycle (IDC). The motor is designed considering various rotor pole permanent magnet shapes keeping the geometrical dimensions identical. Parametric analysis is applied to select optimal shape of the rotor pole by varying the embrace factor and magnet thickness which provides reduced torque ripples with optimized performance parameters. Ansys Maxwell software is used for the adaptive FEA of the designed PMSM model.

2. Dynamic Equations of Three-Wheeler EV

BEV should be capable of overcoming the resistive force(s) to propel the wheels. The movement of the vehicle could be described by motion, torque, power, and related parameters could be calculated with these equations. The total resistive force is the combination of the aerodynamic force, rolling resistive force, Hill climbing force, and acceleration force is represented in the Eq. (1). The power and torque equation of the vehicle is represented as in Eq. (2) and Eq. (3) [31, 32]. The pre-defined parameter values for three-wheeler electric vehicles are mentioned in Table 1 [20]. In the equations F_t is the tractive force; ψ is the slope angle of vehicle, g is the gravity, A is the frontal area of vehicle, v is the velocity, a is the acceleration of vehicle, T_t is the tractive torque and P_t is the tractive power of the vehicle. The applied resistive forces and other constraints on a three-wheeler are shown in Fig. 1.

$$F_t = \frac{1}{2}\rho\, A\, C_d v^2 + M\, g\, \mu_{rr}\, Cos\psi + M\, g\, Sin\psi + M\, a \quad (1)$$

$$T_t = F_t * r \quad (2)$$

$$P_t = F_t\, v \quad (3)$$

Table 1. Specifications of the BEV.

Parameter	Value
Total weight *(M)*	475 kg
Density of air *(ρ)*	1.225
Drag coefficient *(C_d)*	0.5575
Rolling resistance coefficient *(μ_{rr})*	0.015
Diameter of wheel *(d)*	10 inches

The graphical representation of the Indian driving cycle (IDC) which is the graphical image of velocity vs time is shown in Fig. 2. The value of gradient force is negligible on flat roads. The acceleration force is constant when vehicles run on

the sloppy road. From dynamic equations the resultant frictional torque and other desired parameters are determined. The designed motor is generally driven for low speed. The speed is 25 kmph and maximum acceleration is 6.94 m/s^2. The speed at the slope of 8° is considered one third of the maximum speed and the acceleration force remains constant.

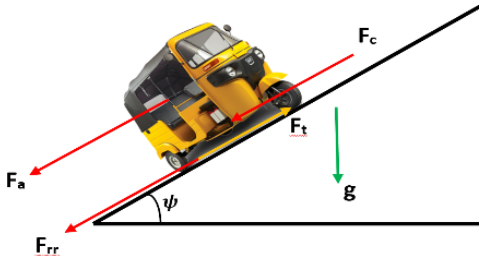

Fig. 1. Resistive forces acting on a three-wheeler.

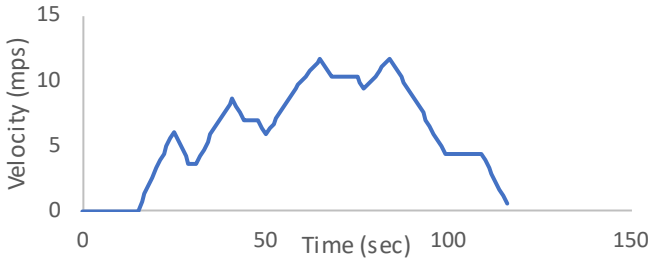

Fig. 2. Indian driving cycle.

The graphical representation of acceleration with time is shown in Fig. 3. The main indices of the motor considered are rated power, rated speed and rated torque i.e., 2 kW, 1500 rpm and 12.7 Nm.

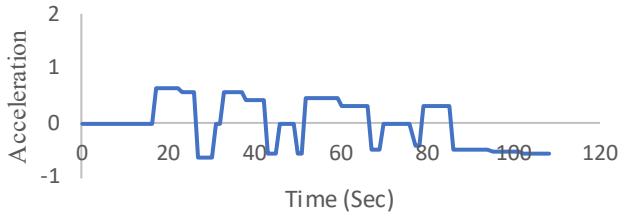

Fig. 3. Acceleration of IDC.

3. Mathematical Equations of PMSM

The rotor of the PMSM has radially magnetised and alternately pole magnets. The electromagnetic torque (T_{em}) of a motor is the sum of the reluctant torque (T_{re}) and magnet torque (T_{pm}) as mentioned in Eq. (4). The reluctant torque is computed using Eq. (5), where currents are the per-phase rms quantities and p is the rotor pole pairs. From the magnet structure, it can be observed that the magnet path seen by the

currents from the d-axis and q-axis is different. Saliency is the magnetic axis physically and magnetically stand out or apart from one another. It is the ratio of the inductance on the q-axis to the d-axis presented in Eq. (6). The value of saliency (*S)* is greater than unity for the Interior type of permanent magnet motor but equal to unity in Surface permanent magnet motor [33, 34].

$$T_{em} = T_{pm} + T_{re} \tag{4}$$

$$T_{re} = \frac{3}{2}p\left[\lambda_m i_q + \left(L_d - L_q\right)i_d i_q\right] \tag{5}$$

$$S = {L_q}\Big/{L_d} \tag{6}$$

From the equation i_q and i_d are the per phase rms currents along quadrature axis and direct axis, λ_m is the magnet flux linkage, L_d, L_q is the magnetizing inductance along direct and quadrature axis. The flux linkage of the motors in the d and q axis can be defined by Eq. (7) and Eq. (8). The steady state IPM motor stator voltage equations written in the d-q rotating reference frame are presented in Eq. (9) and Eq. (10).

$$\lambda_d = L_d I_d + \lambda_m \tag{7}$$

$$\lambda_q = L_q I_q \tag{8}$$

$$v_d = R i_d - w L_q i_q \tag{9}$$

$$v_q = R i_q + w L_d i_d + w\lambda_m \tag{10}$$

where, i_d, i_q, v_d, v_q are the d- and q- axis components of the armature current and terminal voltage, respectively. *R* is the winding resistance per phase, L_q, L_d are the inductances along d- and q- axis, *w* is the electrical speed and λ_m is the magnet flux linkage with d-axis armature winding [34]. The equivalent diagram is shown in Fig. 4.

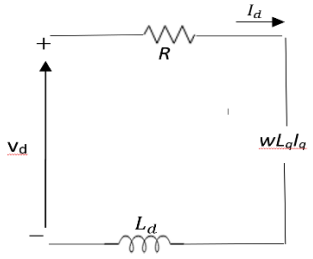

Fig. 4. Equivalent diagram of d-axis of PMSM.

The electromagnetic power P_{em} is given by Eq. (11). The input power is the sum of ohmic loss and electromagnetic power presented in Eq. (12).

$$P_{em} = 3E_{ph}I_q + 3w(L_d - L_q)I_d I_q \tag{11}$$

$$P = 3R\left(I_q^2 + I_d^2\right) + P_{em} \tag{12}$$

E_{ph} is per phase back emf and *R* is the winding resistance per phase. The torque ripple termed as T_{ripple} can be calculated with the help of Eq. (13). The torque ripples are calculated for the peak-to-peak torque of the motor where T_{max} is the maximum torque, T_{min} is the minimum torque and T_{avg} is the average torque [34].

$$T_{ripple} = \frac{T_{max} - T_{min}}{T_{avg}} * 100 \quad (13)$$

The efficiency of the motor is presented in Eq. (14) where P_i is the input power and P_o is the output power [34].

$$\eta = \frac{P_o}{P_i} * 100 \quad (14)$$

4. Design specifications of the PMSM

For e-rickshaw the PMSM has been designed on the RMxprt platform of Maxwell software. Considering the prerequisite data for the design, the motor has been selected as a work case for the EV [20]. The dimensional specification of the model is mentioned in Table 2. The stator part of the motor is made of steel M19_24G because it produces less core losses as compared to other materials of steel grades. The stator winding is made of copper because of its good conductivity. The permanent magnet material is of NdFe35 because of its better magnetic flux density 1.23 Tesla (T). The initial value chosen for the variables pole embrace factor and magnetic thickness is 0.9 and 3 mm. The general diagram of the reference model of PMSM is shown in Fig. 5. This refers to the overview of radial type rotor pole PM shaped PMSM.

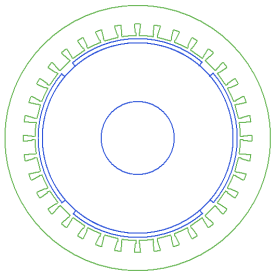

Fig. 5. Geometrical Overview of the radial type of PM shape PMSM.

Table 2. Dimensional specifications of PMSM.

Particulars	Values
Stator outer diameter (D_{so})	179 mm
Stator inner diameter (D_{si})	138.5 mm
Rotor inner diameter (D_{ri})	50 mm
Stack length (L)	108 mm
No. of pole/slot (N_{ps})	4/36
Frequency (f)	50 Hz
Voltage (V)	220V
Speed (N)	1500 rpm
Power (P)	2 kW
Torque (T)	12.7 Nm

5. Comparative Analysis of Rotor Models

The design of the rotor and the placement of the permanent magnets significantly affects the motor characteristics. In the analysis, four different types of rotor poles permanent magnet (PM) shapes of the PMSM are considered. The general overview of the motor of various rotor pole shapes is shown in the Fig. 6. The

designed model of PMSM has 4 poles and 36 slots, which is analysed for the constant power at speed of 1500 rpm. High efficiency, low cogging torque component, less cost and compact size of motor may be regarded as the important criteria that should be considered for the optimum design. In this respect, some performance metrics are examined, including motor efficiency, cogging torque amplitude, and quantity of magnet consumption. The derived results are compared in Table 3 for the performance analysis of the various rotor pole shapes of the motor. The step-by-step process of adaptive FEM is shown in *appendix A-1*.

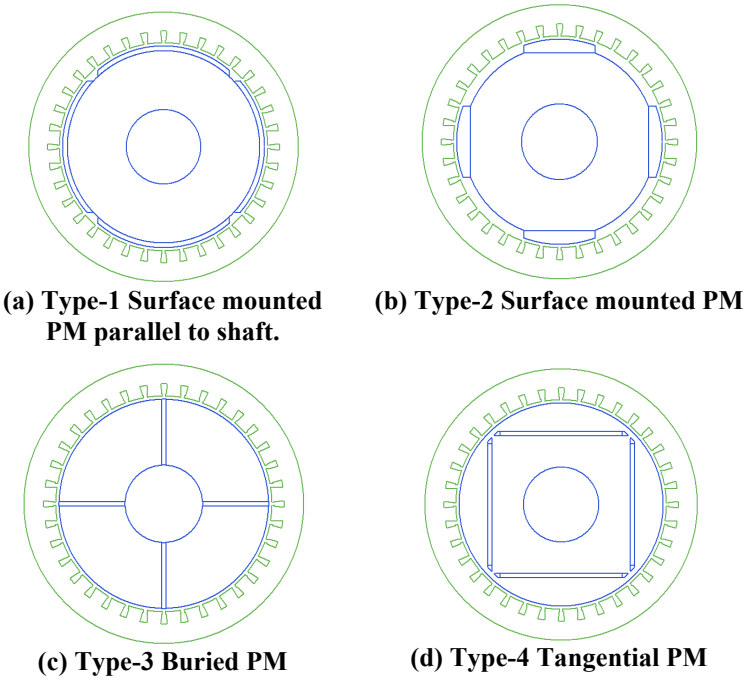

(a) Type-1 Surface mounted PM parallel to shaft.

(b) Type-2 Surface mounted PM

(c) Type-3 Buried PM

(d) Type-4 Tangential PM

Fig. 6. Proposed types of rotor pole PM of motor.

Table 3. Comparative analysis of the rotor pole shapes of PMSM.

Parameters	Type-1	Type-2	Type-3	Type-4
Average Current (A)	10.4	10.06	19.42	10.5
Efficiency (%)	87.3	90.3	71.9	86.3
Cogging Torque (Nm)	0.41	0.49	0.59	0.45
Output Power (W)	2000.4	2000.13	1587.3	2000.3
Torque (Nm)	13.38	12.62	13.8	13.2
Speed (rpm)	1427	1513	1094	1445.69
Air gap flux density (T)	0.46	0.83	0.32	0.44
PM Weight (kg)	0.92	1.14	0.33	0.77

According to the data, Type-3 design, when compared to the other designs, gives the lowest efficiency, speed, and the highest cogging torque component. Since reduction of cogging torque is an important and crucial factor therefore this rotor-magnet structure has not been considered. Although type-2 design has the highest efficiency, but parallelly it has the highest consumption (weight) of

permanent magnets. Overall cost of motor should be affordable. Since the permanent magnets are quite costly therefore its higher consumption in type-2 structure shall make this design economically unviable. Keeping in view the application requirement, the type-1 rotor shape structure is selected for the design of motor as it has lowest cogging torque component, and its electromagnetic torque is also better as compared to type-2 and 4 structures. However, drawback of type-1 design is that its efficiency and speed are less as compared to type-2 and consumption of permanent is more as compared to type-3 and 4. But in terms of the cogging torque and efficiency, type-1 structure is better than type-4. The torque in type-1 is more than required for the propulsion of three-wheeler which is a good sign for selection of this design. Moreover, the significant output power and low value of average current also favour this design. Certain limitations of type-1 design may be compromised keeping in view the prominent advantages and usage.

Parametric Analysis

This section of the study carries out parametric analysis for type-1 design, which has been considered as optimum design based on the application domain. For customizing the design of type-1, parametric analysis has been considered. The embrace factor value is related to the consumption of permanent magnet for a particular design that directly impacts the cogging torque of the motor. The selected design variables are modified in a range while the remaining parameters are kept constant in parametric analysis to obtain the optimum variables for motor design [19]. As a consequence of taking physical limitations into account, the embrace factor is varied from 0.5 to 0.7 to determine the best possible values of design variables. By paying attention to two factors, the first being physical tolerances in magnet production and second being the goal for high sensitivity, the solution step is specified as 0.05. including intermediate values within a step size. Similarly, magnet thickness is varied for the rotor from 5mm to 7 mm having solution step size of 1mm. The electrical parameter assessment of the PMSM model using RMxprt yielded a data set of 25 values of efficiency, torque, and cogging torque at desired speed. For the obtained data sets, parametric analysis has been used to find the best values of design variables to satisfy the performance parameters such as electromagnetic torque, efficiency cogging torque and speed.

The graph related to parametric analysis of variables with performance parameters is shown in Fig. 7. The magnet thickness and embrace factor necessary for the best motor design are found to be 5 mm and 0.8, respectively, by the carried-out simulation studies. By incorporating these numbers into the design, a cogging torque amplitude of 0.598 Nm and an efficiency of 88.42 percent were achieved with necessary torque at rated speed of 1500 rpm. Although efficiency is high at other points, however, speed and torque can't be compromised, so optimum point has been selected accordingly.

6. Finite Element Analysis

After computation of electrical parameters, magnetic field analysis of the motor is also necessary for the holistic overview of electromagnetic field problems. The transient analysis using finite element technique is investigated in this problem. The new motor design for the selected magnet thickness and embrace factor has been proposed subjected to transient finite element analyses at rated load and speed. To simplify the simulation analysis, only $1/4^{th}$ part of the model has been considered.

The mesh plot of the models is shown in Fig. 8. Domain of motor under consideration has been discretized into 2690 first order triangular elements.

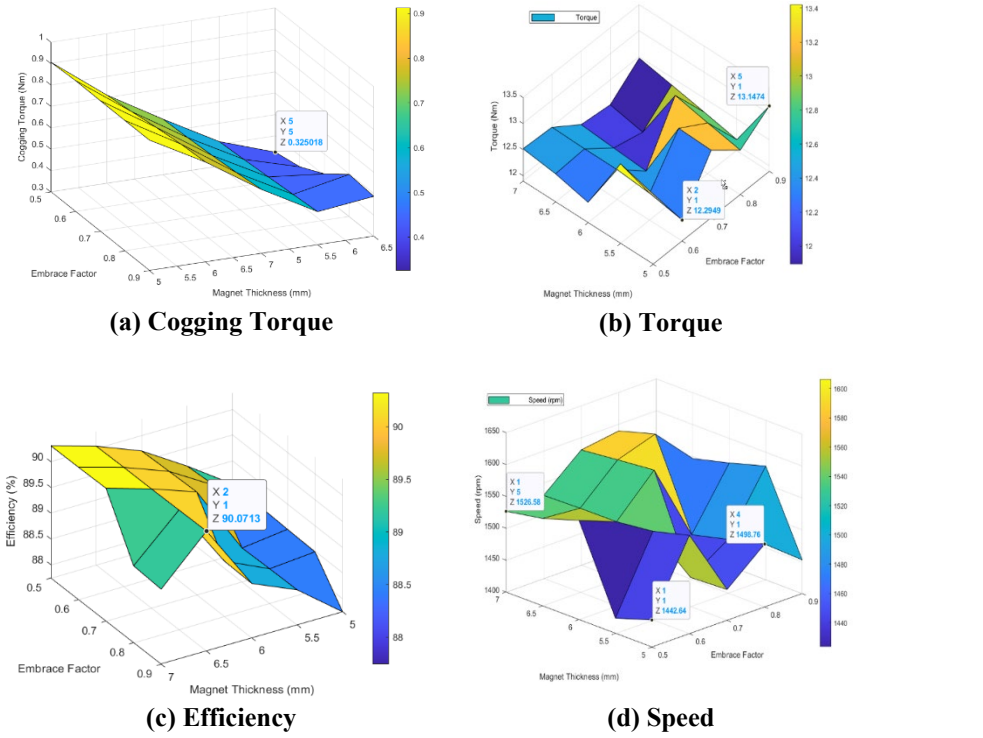

(a) Cogging Torque **(b) Torque**

(c) Efficiency **(d) Speed**

Fig 7. Parametric analysis of cogging torque, efficiency, torque and speed of proposed PMSM model.

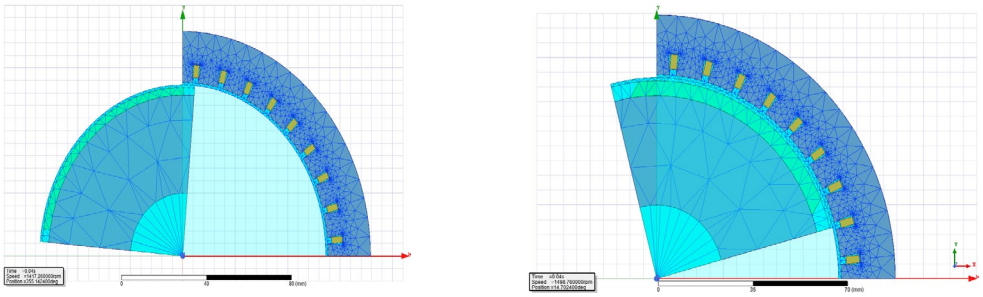

(a) **(b)**

Fig. 8. Finite element mesh of model at different rotor positions.

FEA shows the magnetic field distribution profile at any instant of time and rotor position. The resulting magnetic flux density distribution at different rotor positions are given in Fig. 9.

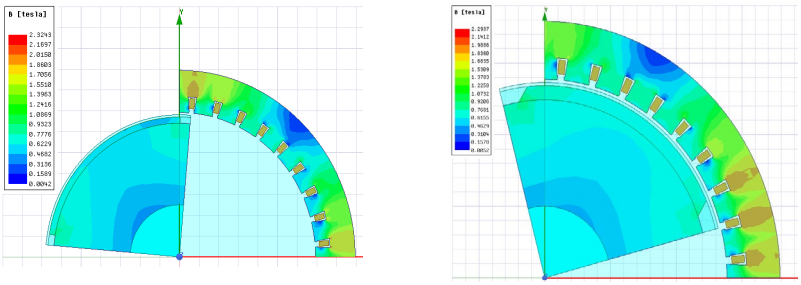

(a) **(b)**

Fig. 9. Magnetic field density distribution at different rotor positions.

The vector based magnetic field intensity of the model at different rotor positions is shown in Fig. 10.

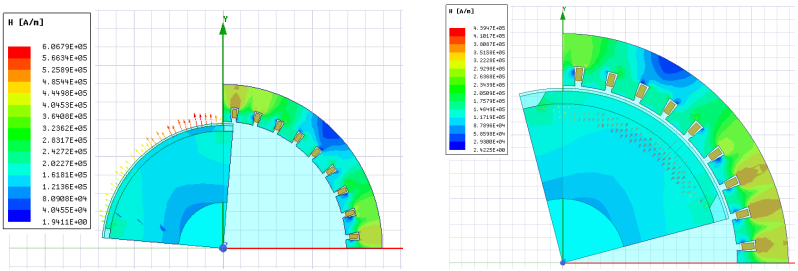

(a) **(b)**

Fig. 10. Magnetic field intensity at different rotor positions.

Transient field analysis of the FEM based models has been done for moving torque response at any instant of time. The electromagnetic torque versus time curve is shown in Fig. 11 of the initial model A and optimal model B. The comparison of the performance parameters between initial model A and optimal model B are mentioned in Table 4. Critical comparison between models in the Table 4 and Fig. 11 illustrates that the optimal model B has less content of torque ripples and other parameters suit the design requirements of three-wheeler BEV. The efficiency of the optimal model B has also increased from 87.3% to 88.4% and significant reduction in torque ripples will increase the life span of the motor with minimum regular maintenance requirement.

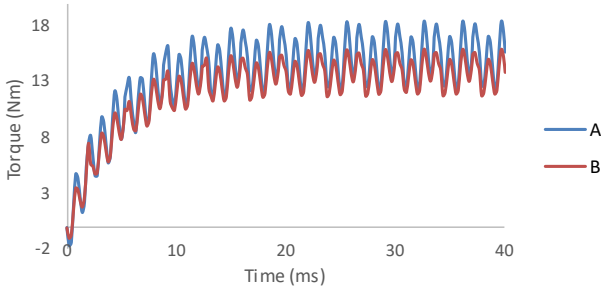

Fig. 11. Variation of electromagnetic torque with time for PMSM.

Table 4. Comparison of various performance parameters.

Parameter	Initial Model A	Optimal model B
Torque (Nm)	13.4	13.3
Efficiency (%)	87.3	88.4
Maximum Torque	18.5	15.91
Minimum Torque	7.9	7.8
Peak to Peak Torque	20.14	16.83
Average Torque	13.62	12.29
Torque Ripple	0.77	0.65

7. Conclusions

The work presented in this research paper shows the impact of various rotor shapes on the performance of the PMSM for the battery electric vehicle. Design type-1 offers optimized performance over other three designs regarding prominent performance parameters: electromagnetic torque, efficiency, and cogging torque of the motor. The influence of magnet thickness and embrace factor has been analysed using parametric analysis. The efficiency of the motor after parametric analysis has increased from 87.3% to 88.4%, in reference to the selected base design. Accordingly, a reduction of 15.5% has been noticed in torque ripple contents in comparison to the initial base design model. The speed and torque ratings of the motor have been matched with the requirements of three-wheeler BEV by selecting the optimum combination of magnet thickness and embrace factor. Reduction in torque ripples indicates less vibrations and acoustic noise which increases the life span as well decreases per litre consumption of three-wheeler BEV.

The present work emphasis mainly on computation of electromagnetic parameters related to electric vehicle. For the holistic analysis of the vehicle, in future, the Multiphysics analysis pertaining to temperature and vibrations may be attempted. Moreover, finite element refinement strategies such as h-type, hp-type may be considered for comparative analysis. Further, an attempt may be made to examine the hierarchal finite element technique on the domain under consideration.

Nomenclatures

A	Frontal Area of wheel
C_d	Aero drag coefficient
D_{ri}	Rotor inner diameter
D_{si}	Stator inner diameter
D_{so}	Stator outer diameter
f	Frequency
F_t	Tractive force
g	Gravity of acceleration
i_d	Armature current in d- axis
i_q	Armature current in q- axis
L	Stack length
L_q	Inductance in q- axis
L_d	Inductance in d- axis
M	Total weight
N	Speed

N_{ps}	No. of pole/slot
P	Power
P_i	Input power
P_o	Output power.
P_t	Tractive power
p	Pole pairs
R	Resistance of winding per phase
R	Radius of tire
S	Saliency
T	Torque
T_{em}	Electromagnetic torque
T_{pm}	Magnet Torque
T_{re}	Reluctant Torque
T_t	Tractive torque
V	Voltage
v	velocity
v_d	Terminal voltage of d-axis
v_q	Terminal voltage of q-axis
w	Electrical speed

Greek Symbols

ρ	Density of air
Ψ	Gradient angle
λ_M	Magnet flux linked
$\mu_{\rho\rho}$	Density of Air

Abbreviations

BEV	Battery Electric Vehicle
EV	Electric Vehicle
FEA	Finite Element Analysis
FEM	Finite Element Method
IDC	Indian Driving Cycle
IPMSM	Interior permanent magnet synchronous motor
PM	Permanent Magnet
PMSM	Permanent magnet synchronous motor
SPMSM	Surface mounter permanent magnet synchronous motor
ZEVs	Zero Emission Vehicles

References

1. Kumar, C.R.J.; and Majid, M.A. (2020). Renewable energy for sustainable development in India: current status, future prospects, challenges, employment, and investment opportunities. *Energy, Sustainability and Society*, 10(2), 1-36.
2. Ghosh, A. (2021). Electric vehicles-solution toward zero emission from the transport sector. *World Electric Vehicle Journal*, 12(4), 1-4.
3. Pellegrino, G.; Vagati, A.; Guglielmi, P.; and Boazzo, B. (2012). Performance comparison between surface-mounted and interior PM motor drives for electric vehicle application. *IEEE Transactions on Industrial Electronics*, 59(2), 803-811.

4. He, C.; and Wu, T. (2016). Design and analysis of a V-type fractional-slots IPMSM with distributed winding for electric vehicles. *Proceedings of the 016 XXII International Conference on Electrical Machines* (*ICEM*), Lausanne, Switzerland, 1459-1465.
5. Jiang, W.; Feng, S.; Zhang, Z.; Zhang, J.; and Zhang, Z. (2018). Study of efficiency characteristics of interior permanent magnet synchronous motors. *IEEE Transactions on Magnetics*, 54(11), 8108005.
6. Sumithra, P.; and Thiripurasundari, D. (2017). A review on computational electromagnetics methods. *Advanced Electromagnetics*, 6(1), 42-55.
7. Zienkiewicz, O.C.; Taylor, R.L.; and Zhu, J.Z. (2005). *The finite element method: its basis and fundamentals.* Elsevier.
8. Sykulski, J.K. (2009). Computational electromagnetics for design optimisation: the state of the art and conjectures for the future. *Bulletin of the Polish Academy of Sciences: Technical Sciences*, 57(2), 123-130.
9. Chan, C.C.; and Chau, K.T. (1991). Design of electrical machines by the finite element method using distributed computing. *Computers in Industry*, 17(4), 367-374.
10. Kumar, A.; Marwaha, S.; and Marwaha, A. (2004). Finite element 2D steady-state time harmonic field analysis of induction motor. *Proceedings of the IEEE INDICON 2004. First India Annual Conference*, Kharagpur, India, 570-574.
11. Kumar, A.; Marwaha, S.; Singh, A.; and Marwaha, A. (2010). Comparative leakage field analysis of electromagnetic devices using finite element and fuzzy methods. *Expert Systems with Applications*, 37(5), 3827-3834.
12. Rupam; and Marwaha, S. (2021). Mitigation of cogging torque for the optimal design of BLDC motor. *Proceedings of the IEEE 2nd International Conference On Electrical Power and Energy Systems (ICEPES)*, Bhopal, India, 1-5.
13. Kumar, A.; Marwaha, S.; Singh, A.; and Marwaha, A. (2009). Performance investigation of a permanent magnet generator. *Simulation Modelling Practice and Theory*, 17(10), 1548-1554.
14. Morin, P.; Nochetto, R.H.; and Siebert, K.G. (2002). Convergence of adaptive finite element methods. *SIAM Review*, 44(4), 631-658.
15. Elamin, M.; and Wendling, P. (2022). NVH analysis of rotor step skewing on permanent magnet synchronous motor. *Proceedings of the 2022 IEEE Transportation Electrification Conference & Expo (ITEC)*, Anaheim, CA, USA, 796-800.
16. Wang, S.C.; Nien, Y.C.; and Huang, S.M. (2022). Multi-objective optimization design and analysis of v-shape permanent magnet synchronous motor. *Energies*, 15(10), 3496.
17. Bdewi, M.Y.; Ali, M.M.E.; and Mohammed, A.M. (2022). In-wheel, outer rotor, permanent magnet synchronous motor design with improved torque density for electric vehicle applications. *International Journal of Electrical and Computer Engineering*, 12(5), 2088-8708.
18. Mersha, T.K.; and Du, C. (2021). Co-simulation and modeling of PMSM based on ansys software and Simulink for EVs. *World Electric Vehicle Journal*, 13(1), 4.

19. Du, G.; Xu, W.; Zhu, J.; and Huang, N. (2019). Effects of design parameters on the multiphysics performance of high-speed permanent magnet machines. *IEEE Transactions on Industrial Electronics*, 67(5), 3472-3483.
20. Murali, N.; Ushakumari, S.; Mini, V.P.; and Varghesee, A.T. (2020). Sizing and performance analysis of an electric motor in an E-rickshaw. *Proceedings of the 2020 IEEE International Conference on Power Systems Technology (POWERCON),* Bangalore, India, 1-6.
21. Li, Y.; Qu, B.; Zhu, Y.; Wan, Y.; and Zhu, X. (2019). Design and analysis of an outer rotor flux switching permanent magnet machine for light electric vehicles. *International Journal of Applied Electromagnetics and Mechanics*, 62(1), 161-172.
22. Chen, H.; Li, X.; Demerdash, N.A.O.; EL-Refaie, A.M.; Chen, Z.; and He, J. (2019). Computationally efficient optimization of a five-phase flux-switching pm machine under different operating conditions. *IEEE Transactions on Vehicular Technology*, 68(7), 6495-6508.
23. Zhang, Z.; Liu, H.; Song, T.; Zhang, Q.; Hu, W.; and Liu, W. (2019). Performance evaluation of a 60kW IPM motor for medium commercial EV traction application. *CES Transactions on Electrical Machines and Systems*, 3(2), 195-203.
24. Ibtissam, B.; Mourad, M.; Medoued, A.; and Soufi, Y. (2018). Multi-objective optimization design and performance evaluation of slotted Halbach PMSM using Monte Carlo method. *Scientia Iranica*, 25(3), 1533-1544.
25. Zhou, T.; and Shen, J.-X. (2017). Cogging torque and operation torque ripple reduction of interior permanent magnet synchronous machines by using asymmetric flux-barriers. *Proceedings of the 2017 20th International Conference on Electrical Machines and Systems (ICEMS)*, Sydney, NSW, Australia,1-6.
26. Li, Y.; Lu, Q.; Zhu, Z.Q.; Wu, D.; and Li, G. (2016). Superposition method for cogging torque prediction in permanent magnet machines with rotor eccentricity. *IEEE Transactions on Magnetics*, 52(6), 8103710.
27. Han, J.-H.; Lee, J.; and Kim, W.-H. (2015). A study on optimal design of the triangle type permanent magnet in IPMSM rotor by using the Box–Behnken design. *IEEE Transactions on Magnetics*, 51(3), 8200704.
28. Huth, G. (2005). Permanent-magnet-excited AC servo motors in tooth-coil technology. *IEEE Transactions on Energy Conversion*, 20(2), 300-307.
29. Lan, I.W.; and Ho, H.-W. (2018). Slot and pole ratio of permanent magnet synchronous motor for cogging torque and torque ripple performance. *Proceedings of the 2018 International Conference of Electrical and Electronic Technologies for Automotive*, Milan, Italy, 1-5.
30. Dhulipati, H.; Mukundan, S.; Ghosh, E.; Li, Z.; Vidalanage, B.G.; Tjong, J.; and Kar, N.C. (2019). Slot-pole Selection for concentrated wound consequent pole PMSM with reduced EMF and inductance harmonics. *Proceedings of the 2019 22nd International Conference on Electrical Machines and Systems (ICEMS)*, Harbin, China, 1-6.
31. Larminie, J.; and Lowry, J. (2012). *Electric vehicle technology explained.* John Wiley and Sons.

32. Omara, A.M.; and Sleptsov, M.A. (2017). Performance assessment of battery-powered electric vehicle employing PMSM powertrain system. *Proceedings of the 2017 IEEE Conference of Russian Young Researchers in Electrical and Electronic Engineering (EIConRus)*, St. Petersburg and Moscow, Russia, 963-968.
33. Huynh, T.A.; and Hsieh, M.F. (2018). Performance analysis of permanent magnet motors for electric vehicles (EV) traction considering driving cycles. *Energies*, 11(6), 1385.
34. Hayes, J.G.; and Goodarzi, G.A. (2018). *Electric powertrain: energy systems, power electronics and drives for hybrid, electric and fuel cell vehicles.* Wiley.

Appendix A

A. 1. Flow sequence of Adaptive FEM

The step-by-step implementation of adaptive FEM is shown in Fig. A-1.

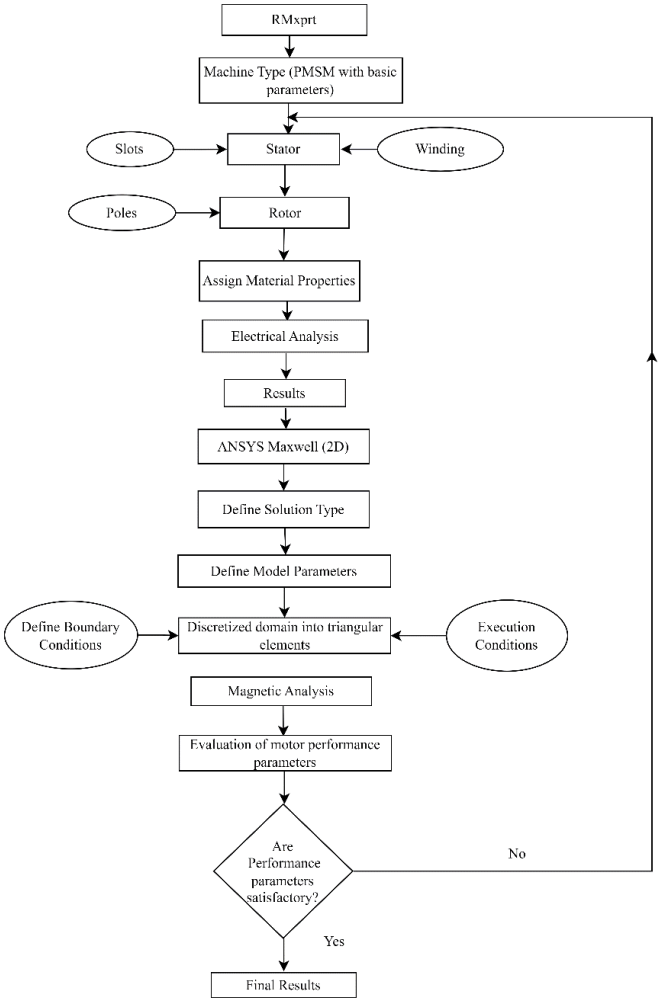

Fig. A-1. Flow sequence of adaptive FEM.